

## RESEARCH ARTICLE

# Imaging of Tumor-Associated Macrophages in a Transgenic Mouse Model of Orthotopic Ovarian Cancer

Huanhuan He,<sup>1</sup> Alan C. Chiu,<sup>1</sup> Masamitsu Kanada,<sup>2</sup> Bruce T. Schaar,<sup>1</sup> Venkatesh Krishnan,<sup>1</sup> Christopher H. Contag,<sup>2,3,4</sup> Oliver Dorigo<sup>1</sup>

<sup>1</sup>Departments of Obstetrics and Gynecology, Stanford University School of Medicine, Stanford, CA, 94305, USA

<sup>2</sup>Departments of Pediatrics, Stanford University School of Medicine, Stanford, CA, 94305, USA

<sup>3</sup>Departments of Microbiology and Immunology, Stanford University School of Medicine, Stanford, CA, 94305, USA

<sup>4</sup>Departments of Radiology, Stanford University School of Medicine, Stanford, CA, 94305, USA

### Abstract

**Purpose:** Tumor-associated macrophages (TAMs) are often associated with a poor prognosis in cancer. To gain a better understanding of cellular recruitment and dynamics of TAM biology during cancer progression, we established a novel transgenic mouse model for *in vivo* imaging of luciferase-expressing macrophages.

**Procedures:** B6.129P2-Lyz2<sup>tm1(cre)flo</sup>/J mice, which express Cre recombinase under the control of the lysozyme M promoter (LysM) were crossed to Cre-lox Luc reporter mice (RLG), to produce LysM-LG mice whose macrophages express luciferase. Cell-type-specific luciferase expression in these mice was verified by flow cytometry, and via *in vivo* bioluminescence imaging under conditions where macrophages were either stimulated with lipopolysaccharide or depleted with clodronate liposomes. The distribution of activated macrophages was longitudinally imaged in two immunocompetent LysM-LG mouse models with either B16 melanoma or ID8 ovarian cancer cells.

**Results:** *In vivo* imaging of LysM-LG mice showed luciferase activity was generated by macrophages. Clodronate liposome-mediated depletion of macrophages lowered overall bioluminescence while lipopolysaccharide injection increased macrophage bioluminescence in both the B16 and ID8 models. Tracking macrophages weekly in tumor-bearing animals after intraperitoneal (i.p.) or intraovarian (i.o.) injection resulted in distinct, dynamic patterns of macrophage activity. Animals with metastatic ovarian cancer after i.p. injection exhibited significantly higher peritoneal macrophage activity compared to animals after i.o. injection.

**Conclusion:** The LysM-LG model allows tracking of macrophage recruitment and activation during disease initiation and progression in a noninvasive manner. This model provides a tool to visualize and monitor the benefit of pharmacological interventions targeting macrophages in preclinical models.

**Key words:** Macrophages, Bioluminescence, Transgenic mice, Ovarian cancer

Electronic supplementary material The online version of this article (doi:[10.1007/s11307-017-1061-2](https://doi.org/10.1007/s11307-017-1061-2)) contains supplementary material, which is available to authorized users.

Correspondence to: Oliver Dorigo; e-mail: odorigo@stanford.edu

### Introduction

Macrophages are a major component of the innate immune system and play important roles in both inflammation and tissue repair [1]. In the context of cancer, the presence of

infiltrating tumor-associated macrophages (TAMs) in cancer tissue is often correlated with poor patient prognosis [1–3]. TAMs represent the most abundant immune population present in human ovarian tumors and ascites [4]. It has been shown in ovarian cancer, and other cancer types, that TAMs can aid cancer progression by supporting tumor cell growth, invasion, angiogenesis, and creating an immunosuppressive microenvironment [5–8].

Macrophages in normal and cancer tissues can be categorized into two distinct subtypes, M1 (classically activated) and M2 (alternatively activated) [1]. M1 macrophages enhance immune responses and restrain tumor progression. In contrast, M2 macrophages and related myeloid cells (Tie2+ monocytes and myeloid-derived suppressor cells) suppress antitumor immune responses and promote tumor development and angiogenesis [1]. TAMs found in cancer patient samples are predominantly polarized to M2 phenotype [9, 10]. The polarization status of TAMs is most likely due to dynamic signaling from the tumor microenvironment [11, 12].

The spatiotemporal dynamics of macrophage recruitment during cancer progression has been investigated using MRI and iron oxide (ferroxidite) labeled M1 and M2 cells [13, 14]. However, due to the lack of a genetic tag, these noninvasive assays in preclinical models have been limited to short-term studies. Lysozyme M (LysM) is expressed exclusively in myeloid lineages, with the highest levels of expression in macrophages and neutrophils [15, 16], and its promoter serves as a regulatory element for selective expression in these cell types. Transgenic mice expressing Cre recombinase from the LysM promoter can be used as a differentiation marker to tag myeloid cells *in vivo*. For the purpose of tagging and imaging macrophages in living subjects, we used B6.129P2-Lyz2<sup>tm1(cre)lfo</sup>/J mice that express Cre recombinase under the LysM promoter (LysM-Cre) to confer reporter gene expression on myeloid cells. These mice were crossed to a Cre-LoxP luciferase reporter mouse strain in which the reporter gene (RLG; loxP-Renilla luciferase-STOP-loxP-red click beetle luciferase-green fluorescent protein) expression is driven by a strong, constitutive hybrid CAG promoter composed of the chicken β-actin promoter and the immediate early enhancer from cytomegalovirus (CMV) [17, 18]. The resulting f1 mice from this cross, called LysM-LG mice, have a B6-FVB hybrid background and should only express click beetle luciferase in myeloid cells in which the LysM promoter is, or had been, active. We used the f1 mice from this cross as hosts for the B16 (melanoma) and ID8 (ovarian) cancer cell lines and monitored myeloid cell activation and proliferation patterns using *in vivo* bioluminescence imaging (BLI).

## Materials and Methods

### *Generation of LysM-LG Transgenic Mice*

B6.129P2-Lyz2<sup>tm1(cre)lfo</sup>/J mice (LysM) were purchased from The Jackson Laboratory, ME, USA (004781). We created the RLG mice as an activatable reporter line, and these have been previously described [17, 18]. All mice were maintained in an

American Association for the Accreditation of Laboratory Animal Care-accredited animal facility. All applicable institutional and/or national guidelines for the care and use of animals were followed. All protocols were approved by the Stanford University Institutional Animal Care and Use Committee under protocol APLAC-28335.

### *In Vivo Models of Ovarian Cancer and Melanoma*

We used the f1s of the LysM-RLG genetic cross such that we could study myeloid cells in immunocompetent murine models of ovarian cancer and melanoma on a compatible genetic background. The B6-derived ovarian cancer cell line, ID8, was cultured in DMEM containing 4 % FBS (Atlanta Biologics), 1 % penicillin/streptomycin (Sigma), and 1 % insulin-transferrin-selenium (Sigma). This cell line was used to create a metastatic model by injecting  $5 \times 10^6$  cells i.p. (in 100 µl phosphate-buffered saline (PBS)) into each mouse. The orthotopic cancer model was initiated by injecting  $4 \times 10^5$  cells (in 5 µl PBS) into one ovary (intraovarian (i.o.)) of each mouse. The end stage is defined as decreased mobility due to ascite-induced abdominal distention. All animals were sacrificed at 12–13 weeks to keep the time of evaluation consistent.

For the melanoma model, the B6-derived B16 melanoma cells were cultured in DMEM containing 10 % FBS (Atlanta Biologics), 1000 U/ml penicillin, 1 mg/ml streptomycin (Sigma), then injected subcutaneously (s.c.) into the dorsal side of the upper hind limb of LysM-RLG mice at a dose of  $1 \times 10^6$  cells in 100 µl PBS. Animals were sacrificed at the indicated time before tumors were ulcerated. All protocols were approved by the Stanford University Institutional Animal Care and Use Committee under protocol APLAC-28518.

### *Bioluminescence Imaging (BLI)*

Mice were anesthetized with isoflurane using an inhalation SAS3 anesthesia system (Summit Anesthesia Support) and kept under 2.5 % isoflurane during imaging. D-luciferin (Biosynth) was injected i.p. at 30 mg/kg mouse body weight. Mice were imaged using either the IVIS 100 or 200 (Perkin-Elmer) located in the Stanford University Small Animal Imaging Facility. Both grayscale reference images and bioluminescence images were taken 8 min after injection of D-luciferin, and the bioluminescence image was obtained using an acquisition time of 30 s.

For *in vitro* BLI, D-luciferin (30 mg/ml) was added (in 1:100 dilution) to PBS containing either whole organs or sorted cells. An IVIS 100 (Perkin-Elmer) was used for imaging. Images were acquired 10 min after adding D-luciferin with a 1-min integration time.

For image analysis, the pseudo-color representations of the bioluminescent signals were superimposed over the grayscale photographic images using Living Image software (Perkin-Elmer). The same ROI was used for all the animals over the abdominal region. Images from the same batch of experiments

were displayed at the indicated ranges of radiance. Average radiance ( $\text{p/sec/cm}^2/\text{sr}$ ) was used for quantifications.

### In Vivo Manipulation of Macrophages

For liposome depletion of macrophages, 100  $\mu\text{l}$  of clodronate (Clodronate Liposomes, Netherlands) or control (PBS) liposomes were injected IV daily. In the B16 model, clodronate or control liposome treatment started on day 8 post-tumor inoculation and bioluminescent signals were evaluated daily for two consecutive days. In the ID8 i.p. model, clodronate or control liposome treatment was initiated 7 weeks after tumor inoculation, and bioluminescent signals were evaluated daily for three consecutive days.

For lipopolysaccharide (LPS) experiments, each animal was treated with 100  $\mu\text{l}$  of 1 mg/ml LPS or PBS via i.p. injection. Bioluminescent signals were evaluated 16 h after treatment. Peritoneal macrophages were harvested via peritoneal lavage and stained for flow cytometry analysis.

### Isolation and Culture of Peritoneal Macrophages

Peritoneal cells were collected after peritoneum lavage using PBS. Cells were plated on six-well cell culture plates and maintained in DMEM medium containing 10 % FBS (Atlanta Biologicals), 1 % penicillin/streptomycin (Sigma), and 10 ng/ml murine M-CSF (Peprotech) for 6 days. Cells were then polarized with either 50 ng/ml LPS for 16 h or 10 ng/ml IL-4 for 24 h.

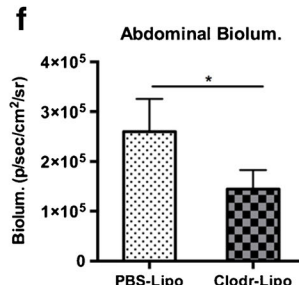
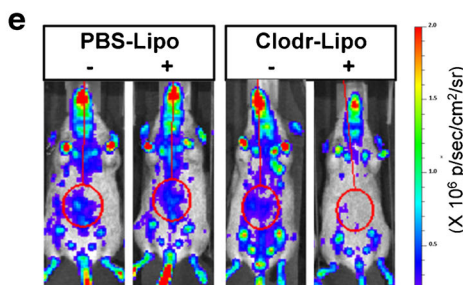
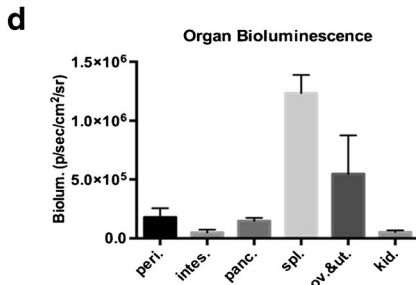
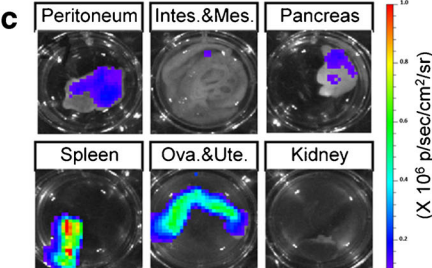
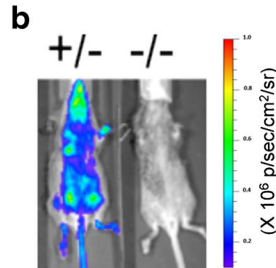
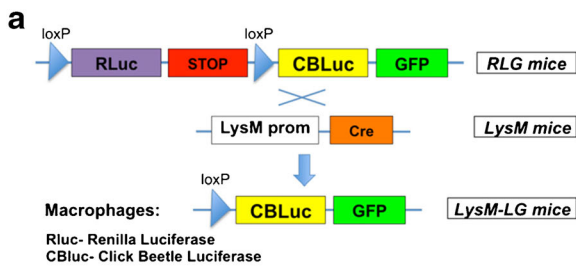


**Fig. 1.** Generation and characterization of LysM-LG macrophage imaging model. **a** Breeding scheme for generating the in vivo macrophage imaging model. **b** Bioluminescent imaging of LysM-LG pups. **c** Representative bioluminescence graphs of organs from LysM-LG mice. **d** Quantification of bioluminescence signal of organs from LysM-LG mice.  $n = 4$ . **e** Bioluminescence images showing that clodronate-liposome treatment reduces bioluminescence in LysM-LG mice. **f** Quantification of abdominal bioluminescence from animals treated with clodronate-liposome and control vehicle (PBS-liposome). PBS-Lipo,  $n = 3$ ; Clodr-Lipo,  $n = 4$ . \* $p < 0.05$  (unpaired Student's *t* test).

### Flow Cytometry Analysis and Cell Sorting

Cells in a single-cell suspension were incubated with fluorophor-conjugated antibodies at 4 °C for 20 min, then resuspended in Flow Cytometry Staining Buffer (eBioscience). Antibodies used were FITC-CD19 (eBioscience), FITC-B220 (eBioscience), eFluor 450-CD11b (eBioscience), APC-Gr1 (eBioscience), APC-iNOS (eBioscience), PE-F4/80 (eBioscience), PE-Cy7-CD11c (eBioscience), and PE-Cy7-CD206 (BioLegend). DAPI (Invitrogen, D1306) was used as cell viability dye. LSRII Analytic Flow Cytometer (BD) was used for acquisition. BD FACSAria™ cell sorter was used for cell sorting. Data was analyzed with FlowJo (Tree Star, Inc.).

## Results

### Generation and Characterization of LysM-LG Transgenic Mice

We generated a transgenic mouse model for that would enable dynamic in vivo imaging of tumor-associated macrophages. Cre-lox Luc reporter mice (RLG) were crossed to B6.129P2-Lyz2<sup>tm1(cre)Ifo</sup>/J mice (LysM; Fig. 1a). RLG mice express click beetle luciferase (CBLuc) after Cre recombinase-mediated deletion of a floxed Renilla luciferase and translational stop sequence including a polyadenylation signal sequence. The LysM mice produce Cre recombinase under the control of the lysozyme 2 promoter, which is exclusively active in myeloid cells

including macrophages [15, 16]. The f1 offspring of this cross produced robust bioluminescence that could be visualized *in vivo* using In Vivo Imaging System (IVIS) [19, 20] (Fig. 1b) and are on the combined background of FVB and B6 such that they can accept B6-derived tumors. Regions of the LysM-LG mice expressed different levels of luciferase with the highest intensity observed over an area corresponding to the spleen (Fig. 1c, d). The expression of bioluminescence from macrophages has been confirmed by flow sorting macrophages followed by luminometer analysis (Suppl. Fig. 1a). Depletion of macrophages using injection of clodronate-liposomes decreased the bioluminescent signal by 44.4 % (Fig. 1e, f; Suppl. Fig. 1b).

### Enhanced Bioluminescence Signal in Activated Macrophages

After establishing the baseline expression of luciferase of macrophages obtained from LysM-LG animals, we studied bioluminescent signals after activation with

LPS. Overall, the animals injected with LPS showed enhanced bioluminescent signals compared to the control group (Fig. 2a; Suppl. Fig. 2a, b). The signals from the abdomen of the LPS-stimulated animals increased ~2.5-fold compared to the signals detected from the same regions of control animals (Fig. 2b). Evaluation of bioluminescence intensity from cells collected via peritoneal lavage confirmed the elevated signals in macrophages upon LPS stimulation (Fig. 2c). Flow cytometry analysis for activated macrophage markers, inducible nitric oxide synthase (iNOS) and the mannose receptor (CD206) [21–23] on peritoneal macrophages detected a significant increase of activated macrophages in LPS-injected mice (Fig. 2d) with a higher M1/M2 ratio compared to control animals (Fig. 2e).

### Imaging Macrophages in Murine Ovarian Cancer Model (ID8 IP)

The dynamics of TAM infiltration into the peritoneal cavity of immunocompetent mice with ID8 ovarian cancer cells

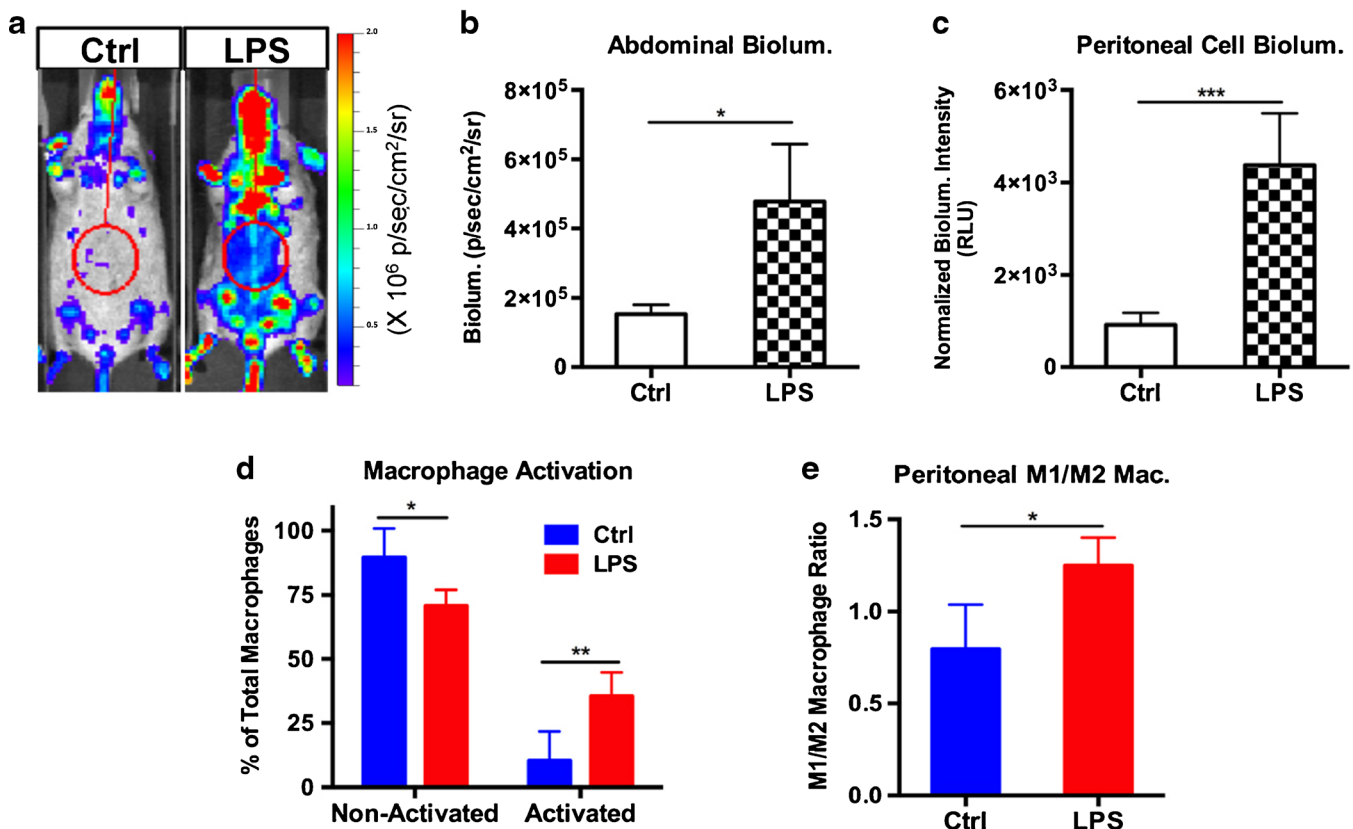


**Fig. 2.** Enhanced bioluminescence signal in activated LysM-LG macrophages. **a** LPS treatment of LysM-LG mice induces bioluminescence in LysM-LG mice. Ctrl, PBS. **b** Quantification of abdominal bioluminescence in LPS-treated animals and control group. Ctrl, PBS.  $n = 3$ . **c** Luciferase activity by equal number of cells harvested from peritoneal cavity of LPS or control (Ctrl, PBS) treated animals.  $n = 4$ . **d** Quantification of macrophage activation by flow cytometry analysis. Activated macrophages were detected by either iNOS or CD206. Ctrl,  $n = 4$ ; LPS,  $n = 3$ . **e** Ratio of M1 and M2 macrophages in peritoneal lavage by flow cytometry analysis. M1, iNOS positive. M2, CD206 positive. Ctrl,  $n = 3$ ; LPS,  $n = 4$ . \* $p < 0.05$ ; \*\* $p < 0.01$  (unpaired Student's *t* test).

growing i.p. were evaluated using BLI. ID8 cells were injected i.p. into LysM-LG mice, and the animals were followed by BLI to assess the development of abdominal TAMs, and were monitored for the presence of ascites. Weekly bioluminescence imaging showed a significant increase in luciferase signal intensity over time with peak signals at 12 to 13 weeks after tumor inoculation (Fig. 3a, b). Increases in bioluminescence were confirmed in excised tissues including the peritoneum, intestines, pancreas spleen, ovary, uterus, and kidneys in these animals (Suppl. Fig. 3a, b). The increase of abdominal signal was associated with an expanded macrophage population (Fig. 3c). Evaluation of the polarization status of peritoneal macrophages identified M2-polarized macrophages via CD206 expression as the major contributors to the increased signal, whereas the M1-polarized macrophages, marked by iNOS expression, were barely detectable (Fig. 3d, e). The predominance of M2 macrophages in the ID8 tumor ascites had been previously demonstrated by us [24].

### Longitudinal Tracking Macrophages in Murine Ovarian Cancer and Melanoma Models

To monitor the progression of macrophage infiltration and proliferation in the presence of ovarian cancer, mice that had received ID8 cells were longitudinally and noninvasively assessed by BLI over a 12-week period (Fig. 4a). One week post-injection of ID8, there was a significant increase in bioluminescent signal. Over the following 11 weeks, the signal plateaued with a marked increase at week 12 (Fig. 4b).

We next explored potentially distinct recruitment or activation of macrophages after orthotopic, i.o. injection of ID8 cells compared to i.p. injection. LysM-LG animals underwent i.o. injection of ID8 cells were followed by weekly bioluminescence imaging to monitor macrophages (Fig. 4c). We observed an overall weaker bioluminescence signal throughout the development of intra-abdominal tumor disease. In addition, the bioluminescence peaks as

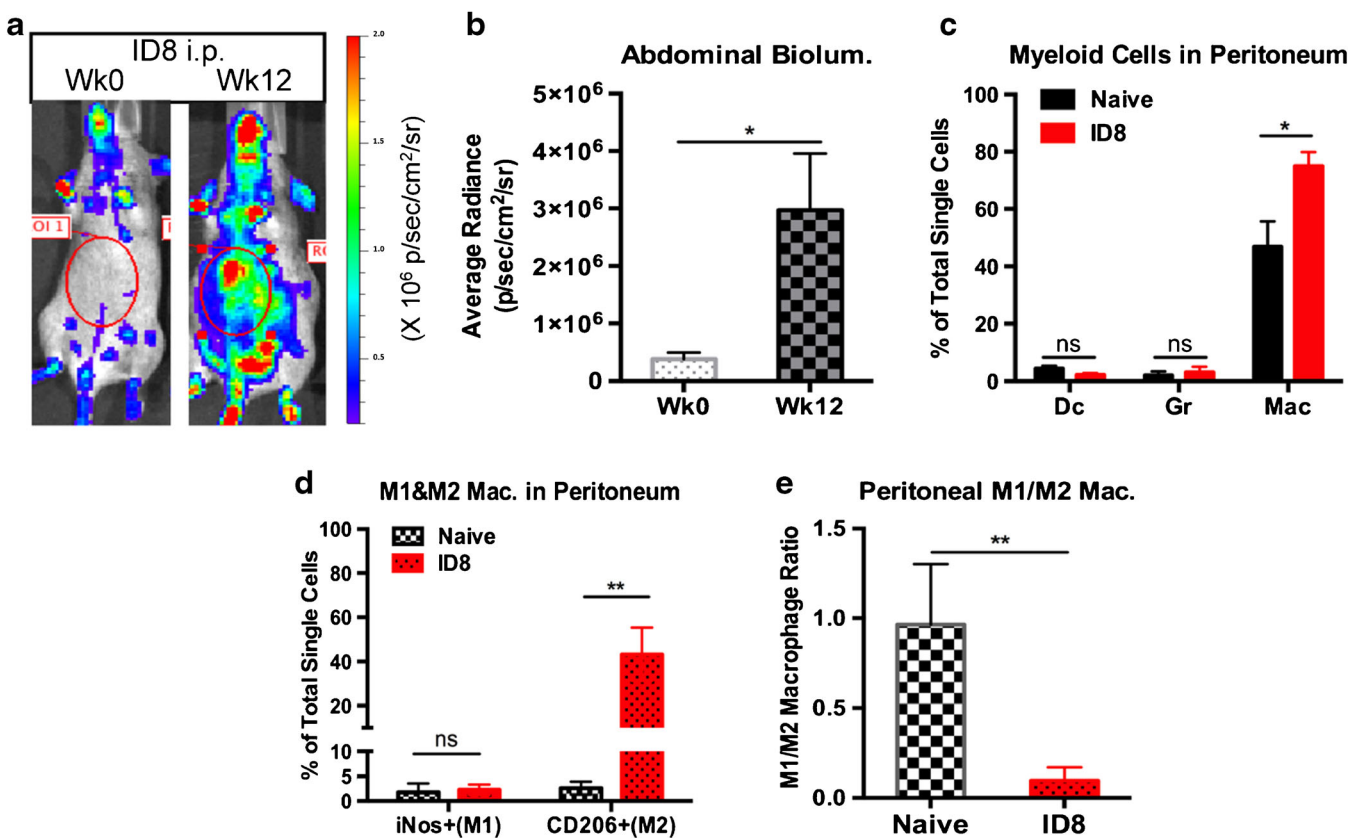


**Fig. 3.** Imaging LysM-LG macrophages in an ID8 i.p. ovarian cancer. **a** Representative bioluminescence images of LysM-LG mice injected (i.p.) with  $5 \times 10^6$  ID8 cells that developed murine ovarian cancer. **b** Quantification of bioluminescence signals from the abdomen of ID8 (i.p.) LysM-LG animals before and after disease. W0,  $n = 5$ ; W12,  $n = 4$ . **c** Quantification of myeloid cell populations in peritoneal lavage (naive) or ascites (ID8) by flow cytometry. Dc dendritic cells (CD11c+), Gr granulocytes (Gr-1+), Mac macrophages (F4/80+).  $n = 3$ . **d** Quantification of polarized macrophages in peritoneal lavage (naive) or ascites (ID8) by flow cytometry. Markers for polarized macrophages are indicated.  $n = 4$ . **e** Ratio of M1 and M2 macrophages in peritoneal lavage (Naive) and ascites (ID8) by flow cytometry analysis. M1, iNOS positive. M2, CD206 positive.  $n = 4$ . \* $p < 0.05$ ; \*\* $p < 0.01$  (unpaired Student's *t* test).

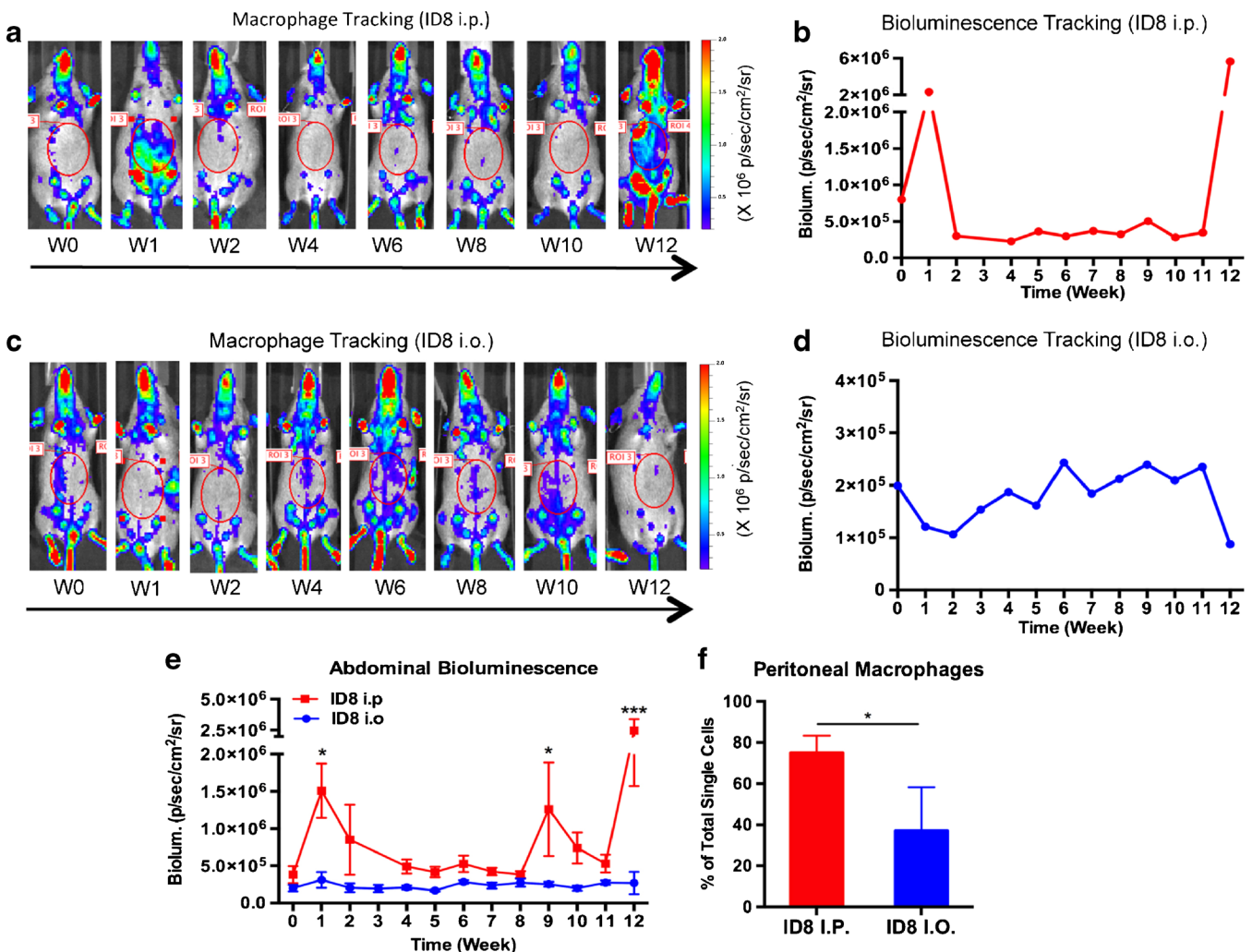


**Fig. 4.** Longitudinal tracking of LysM-LG macrophages in murine ovarian cancer models - either i.p. or i.o. Bioluminescent images of a LysM-LG mouse received **a** i.p. or **c** i.o. injection with ID8 ovarian cancer cells. Abdominal bioluminescence signals from ID8 **b** i.p. or **d** i.o. animals shown in **a** or **c**, respectively. **e** Comparison of bioluminescence signals at the indicated time points between LysM-LG animals injected with ID8 via i.p. versus i.o.  $n = 4$  for i.o.;  $n = 5$  for i.p.. \* $p < 0.05$ ; \*\*\* $p < 0.0001$  (Sidak's multiple comparisons test). **f** Quantification of macrophage percentage in peritoneum by flow cytometry analysis. Macrophages were detected by F4/80 expression.  $n = 4$ . \* $p < 0.05$  (unpaired Student's *t* test).

observed in the i.p. model were not present (Fig. 4d, e). The peaks of bioluminescence in the i.p. model represent macrophage activation/accumulation, which was confirmed by the flow cytometry analysis in the peritoneal lavage at the end point (Fig. 4f).

Macrophage activity was also examined in the B16 model of melanoma. B16 melanoma cells were injected subcutaneously (s.c.) on the backs of LysM-LG mice. In vivo bioluminescence imaging was performed every other day due to the rapid progression of this disease (Suppl. Fig. 4a) and quantitated as described previously (Suppl. Fig. 4b). Similar to the ID8 i.p. model, we observed an increase in bioluminescence during the development of s.c. tumor indicating an increased influx of macrophages during tumor growth (Suppl. Fig. 4c).

#### Monitoring Macrophage Depletion in Tumor-Bearing LysM-LG Mice

In order to examine the contribution of macrophages to the bioluminescence signal, clodronate liposomes were injected to deplete macrophages in both ID8 ovarian cancer and B16 melanoma models. The liposome treatment in the ID8 i.p. ovarian cancer model was initiated at week 7 (Fig. 5a, b) and was repeated daily for 3 days. The signal was reduced by 70.8 % after 3 days (Fig. 5c). For the B16 model, clodronate-liposomes were injected when the bioluminescence of the tumor area was clearly distinguishable from the background 8 days after tumor inoculation (Fig. 5d, e). The signal was reduced by 73 % after 48 h (Fig. 5f).

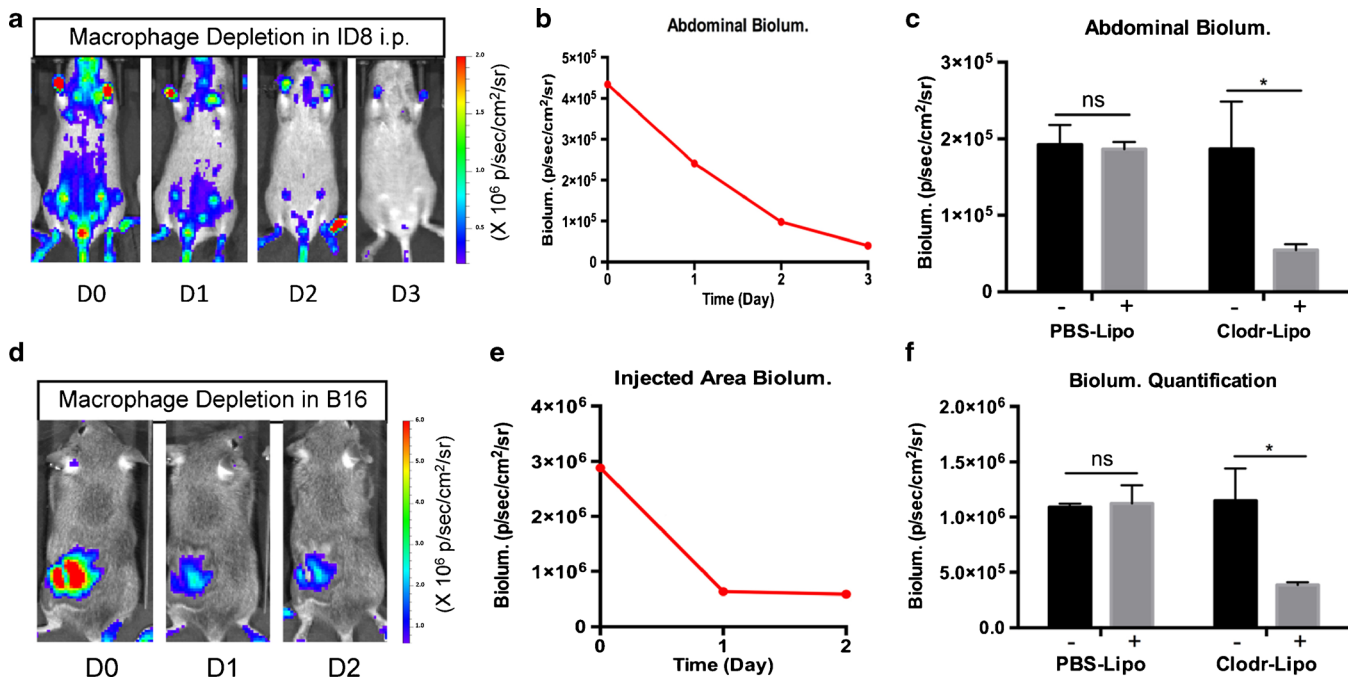


**Fig. 5.** Monitoring macrophage depletion in tumor bearing LysM-LG mice. **a** Representative bioluminescent images of ovarian cancer (ID8 i.p.) in LysM-LG mice that had been treated with clodronate-liposome for three consecutive days. **b** Abdominal bioluminescent signals from the animal shown in **a**. **c** Quantification of bioluminescence from abdominal area of animals after 3 days of clodronate-liposome or control (PBS-liposome) treatment.  $n = 5$ . **d** Representative bioluminescent images of melanoma (B16)-bearing LysM-LG mice treated with clodronate-liposome. **e** Quantification of bioluminescence from injected area of the animal shown in **d**. **f** Comparison of bioluminescence between clodronate-liposome and control (PBS-liposome) groups after 48 h of initial treatment.  $n = 4$ . \* $p < 0.05$  (unpaired Student's *t* test).

## Discussion

Our study describes a useful transgenic mouse model that allows *in vivo* imaging of TAMs in various diseases. This model is useful for the study TAM trafficking during tumor development, and for the investigation of TAM targeting strategies for treatment. TAMs are an important component of the tumor microenvironment [25–31] contributing to tumor progression via different mechanisms including promotion of angiogenesis, enhancing tumor cell invasion, motility, intravasation, and inhibition of antitumor immune responses, and comprise a target for cancer therapy [25, 32–36]. The use of *in vivo* imaging to assess the relative numbers of activated TAMs in the tumor will facilitate the development of effective therapeutic approaches.

We have recently demonstrated that pharmacological TAM targeting can have therapeutic efficacy in the ID8 ovarian cancer model [24]. Macrophage colony-stimulating factor (M-CSF or CSF1) is a potent growth factor that promotes the differentiation, proliferation, and migration of monocytes/macrophages via signaling through the receptor tyrosine kinase CSF1R [37]. CSF-1R signaling is crucial for the survival of the immune-suppressive M2-subtype of macrophages [29]. We used the CSF1R inhibitor GW2480 for the treatment of advanced ID8 tumor disease and observed significant tumor

regression [24]. Tumor regression has also been observed in murine models of glioblastoma multiforme and breast cancer upon treatment with a CSF1-R inhibitor [30, 36]. These studies demonstrate that macrophages are emerging as a promising therapeutic target in cancer. To study the efficacy of macrophage targeting using different therapeutic interventions, the LysM-LG model described here provides a useful tool for the preclinical development of macrophage targeting strategy.

Besides LysM-Cre, various genetic models have been created to target and manipulate macrophages. Promoters of macrophage markers such as macrophage colony-stimulating factor receptor (CSF1R), macrophage scavenger receptor class A (SR-A), and CX3CR1 [26, 27, 31] have been used to drive reporter genes or suicidal genes in order to label or delete macrophage populations. However, CSF1R and CX3CR1 expression are not restricted to macrophages. These receptors are also elevated on the surfaces of monocytes and dendritic cells [28, 38]. LysM-Cre mice have been used in constitutive and conditional gene-targeting studies on myeloid lineages [39, 40]. The fact that luciferase expression driven by the LysM-promoter is much stronger in activated than nonactivated macrophages in our model, is consistent with previous studies of LysM in both mouse and human [41, 42].

In the longitudinal observations of ovarian cancer, two to three peaks of macrophage influx were observed, including one at the initial stage (week 1) and two at the late-stage (weeks 9 and 12). Interestingly, a recent study using the LysM-GFP reporter in spinal cord injury found a similar peak of LysM(+) cells at the beginning of the injury [43]. In this study, these cells obtained larger size morphologically and contained more vacuoles, consistent with activated macrophages. The first observed peak of bioluminescence in this study could be due to an initial inflammatory response after i.p. injection. The observation that peritoneal macrophage activity was more robust in the metastatic model (i.p.) than in the orthotopic model (i.o.) may indicate distinct dynamics of peritoneal macrophage trafficking in these two disease models.

In summary, the LysM-LG model described here provides a useful tool to study when, where and which subtypes of TAMs (activated or nonactivated) are recruited during the course of cancer development, here focusing on ovarian cancer. Future efforts will be made to study the biology of macrophages at different time points of disease development and their responses to pharmacological interventions targeting TAMs.

**Acknowledgements.** This work was supported by the Mary Lake Polan Gynecologic Oncology Endowment for Research (O. D.), the Vivian Scott Fellowship in Gynecologic Oncology (O. D.), the Dean Pizzo Stanford Cancer Center Research Award (O. D.), the Child Health Research Institute at Stanford (C. C.), and a generous gift from the Chambers Family Foundation for Excellence in Pediatric Research (C.C.).

#### Compliance with Ethical Standards

#### Conflict of Interest

The authors declare that they have no conflict of interest.

#### References

- Pollard JW (2009) Trophic macrophages in development and disease. *Nat Rev Immunol* 9:259–270
- De Palma M, Lewis CE (2013) Macrophage regulation of tumor responses to anticancer therapies. *Cancer Cell* 23:277–286
- Cook J, Hagemann T (2013) Tumour-associated macrophages and cancer. *Curr Op Pharm* 13:595–601
- Takaishi K, Komohara Y, Tashiro H et al (2010) Involvement of M2-polarized macrophages in the ascites from advanced epithelial ovarian carcinoma in tumor progression via Stat3 activation. *Cancer Sci* 101:2128–2136
- Gabrilovich DI, Nagaraj S (2009) Myeloid-derived suppressor cells as regulators of the immune system. *Nat Rev Immunol* 9:162–174
- Ostrand-Rosenberg S, Sinha P (2009) Myeloid-derived suppressor cells: linking inflammation and cancer. *J Immunol* 182:4499–4506
- Qian BZ, Pollard JW (2010) Macrophage diversity enhances tumor progression and metastasis. *Cell* 141:39–51
- Solinas G, Marchesi F, Garlanda C et al (2010) Inflammation-mediated promotion of invasion and metastasis. *Cancer Met Rev* 29:243–248
- Mantovani A, Sozzani S, Locati M et al (2002) Macrophage polarization: tumor-associated macrophages as a paradigm for polarized M2 mononuclear phagocytes. *Trends Immunol* 23:549–555
- Zhang M, He Y, Sun X et al (2014) A high M1/M2 ratio of tumor-associated macrophages is associated with extended survival in ovarian cancer patients. *J Ovarian Res* 7:19
- Hagemann T, Wilson J, Burke F et al (2006) Ovarian cancer cells polarize macrophages toward a tumor-associated phenotype. *J Immunol* 176:5023–5032
- Ruffell B, Affara NI, Coussens LM (2012) Differential macrophage programming in the tumor microenvironment. *Trends Immunol* 33:119–126
- Daldrup-Link H, Coussens LM (2012) MR imaging of tumor-associated macrophages. *Oncoimmunology* 1:507–509
- Daldrup-Link HE, Golovko D, Ruffell B et al (2011) MRI of tumor-associated macrophages with clinically applicable iron oxide nanoparticles. *Clin Cancer Res* 17:5695–5704
- Clausen BE, Burkhardt C, Reith W et al (1999) Conditional gene targeting in macrophages and granulocytes using LysMcre mice. *Transgenic Res* 8:265–277
- Cross M, Mangelsdorf I, Wedel A, Renkawitz R (1988) Mouse lysozyme M gene: isolation, characterization, and expression studies. *Proc Natl Acad Sci U S A* 85:6232–6236
- Kanada M, Bachmann MH, Hardy JW et al (2015) Differential fates of biomolecules delivered to target cells via extracellular vesicles. *Proc Natl Acad Sci U S A* 112:E1433–E1442
- Gonzalez-Gonzalez E, Ra H, Hickerson RP et al (2009) siRNA silencing of keratinocyte-specific GFP expression in a transgenic mouse skin model. *Gene Ther* 16:963–972
- Contag CH, Jenkins D, Contag PR, Negrin RS (2000) Use of reporter genes for optical measurements of neoplastic disease in vivo. *Neoplasia* 2:41–52
- Edinger M, Sweeney TJ, Tucker AA et al (1999) Noninvasive assessment of tumor cell proliferation in animal models. *Neoplasia* 1:303–310
- Chow A, Brown BD, Merad M (2011) Studying the mononuclear phagocyte system in the molecular age. *Nat Rev Immunol* 11:788–798
- Lawrence T, Natoli G (2011) Transcriptional regulation of macrophage polarization: enabling diversity with identity. *Nat Rev Immunol* 11:750–761
- Murray PJ, Wynn TA (2011) Protective and pathogenic functions of macrophage subsets. *Nat Rev Immunol* 11:723–737
- Moughon DL, He H, Schokrpur S et al (2015) Macrophage blockade using CSF1R inhibitors reverses the vascular leakage underlying malignant ascites in late-stage epithelial ovarian cancer. *Cancer Res* 75:4742–4752
- Noy R, Pollard JW (2014) Tumor-associated macrophages: from mechanisms to therapy. *Immunity* 41:49–61
- Burnett SH, Kershen EJ, Zhang J et al (2004) Conditional macrophage ablation in transgenic mice expressing a Fas-based suicide gene. *J Leukoc Biol* 75:612–623
- Evrard M, Chong SZ, Devi S et al (2015) Visualization of bone marrow monocyte mobilization using Cx3cr1gfp/+Flt3L−/− reporter mouse by multiphoton intravital microscopy. *J Leukoc Biol* 97:611–619
- Geissmann F, Manz MG, Jung S et al (2010) Development of monocytes, macrophages, and dendritic cells. *Science* 327:656–661
- Hamilton JA (2008) Colony-stimulating factors in inflammation and autoimmunity. *Nat Rev Immunol* 8:533–544
- Pyontek SM, Akkari L, Schuhmacher AJ et al (2013) CSF-1R inhibition alters macrophage polarization and blocks glioma progression. *Nature Med* 19:1264–1272
- Schreiber HA, Loschko J, Karssemeijer RA et al (2013) Intestinal monocytes and macrophages are required for T cell polarization in response to Citrobacter rodentium. *J Exp Med* 210:2025–2039
- Long KB, Beatty GL (2013) Harnessing the antitumor potential of macrophages for cancer immunotherapy. *Oncoimmunology* 2:e26860
- Sica A, Mantovani A (2012) Macrophage plasticity and polarization: in vivo veritas. *J Clin Invest* 122:787–795
- Guiducci C, Vicari AP, Sangaletti S et al (2005) Redirecting in vivo elicited tumor infiltrating macrophages and dendritic cells towards tumor rejection. *Cancer Res* 65:3437–3446
- Ribas A, Wolchok JD (2013) Combining cancer immunotherapy and targeted therapy. *Curr Op Immunol* 25:291–296
- Garris C, Pittet MJ (2013) Therapeutically reeducating macrophages to treat GBM. *Nature Med* 19:1207–1208
- Chitu V, Stanley ER (2006) Colony-stimulating factor-1 in immunity and inflammation. *Curr Op Immunol* 18:39–48
- Sasmono RT, Oceandy D, Pollard JW et al (2003) A macrophage colony-stimulating factor receptor-green fluorescent protein transgene is expressed throughout the mononuclear phagocyte system of the mouse. *Blood* 101:1155–1163

39. Hume DA (2011) Applications of myeloid-specific promoters in transgenic mice support *in vivo* imaging and functional genomics but do not support the concept of distinct macrophage and dendritic cell lineages or roles in immunity. *J Leukoc Biol* 89:525–538
40. Fantin A, Vieira JM, Gestri G et al (2010) Tissue macrophages act as cellular chaperones for vascular anastomosis downstream of VEGF-mediated endothelial tip cell induction. *Blood* 116:829–840
41. Clarke S, Greaves DR, Chung LP et al (1996) The human lysozyme promoter directs reporter gene expression to activated myelomonocytic cells in transgenic mice. *Proc Natl Acad Sci U S A* 93:1434–1438
42. Keshav S, Chung P, Milon G, Gordon S (1991) Lysozyme is an inducible marker of macrophage activation in murine tissues as demonstrated by *in situ* hybridization. *J Exp Med* 174:1049–1058
43. Fenrich KK, Weber P, Rougon G, Debarbieux F (2013) Long- and short-term intravital imaging reveals differential spatiotemporal recruitment and function of myelomonocytic cells after spinal cord injury. *J Physiol* 591:4895–4902